
Heteroepitaxial β -SiC on Si

Y. FURUMURA, M. DOKI, F. MIENO, T. ESHITA, T. SUZUKI, AND M. MAEDA

Fujitsu Limited, Nakahara-ku, Kawasaki 211, Japan





Heteroepitaxial β -SiC on Si

Y. Furumura, M. Doki, F. Mieno, T. Eshita, T. Suzuki, and M. Maeda

Fujitsu Limited, Nakahara-ku, Kawasaki 211, Japan

ABSTRACT

We grew a single crystalline beta silicon carbide (β -SiC) layer at 1000°C on a Si off-axial (111) substrate without using a buffer layer from a gas system of $\text{SiHCl}_3\text{-C}_3\text{H}_8\text{-H}_2$. The heterojunction between epitaxially doped n-type β -SiC and p-type Si showed a diode ideality factor of 1.0-1.1, indicating that β -SiC has a high potential for use as a wide gap emitter material.

Beta silicon carbide (β -SiC) shows promising properties for use in high speed and high power devices working at high temperature. This comes from the physical properties of β -SiC, *i.e.*, a thermal conductivity of 5 W/cm°C, a saturated electron drift velocity of 2×10^7 cm/s, and a breakdown electric field of 3×10^6 V/cm (1). The gap energy of 2.2 eV may be useful in applications using a heterostructure with Si. In order to actually utilize these properties, a large single crystalline wafer is required. However, such a wafer did not exist until Matsunami *et al.* developed a reproducible technique for growing a single crystalline β -SiC layer on a Si substrate at 1330°C using a buffer layer (2-4). That technique made important progress in the reproducible growth of a large area β -SiC on a Si substrate. For practical applications, however, lower growth temperatures are still required.

This paper reports a new technique for growing a single crystalline β -SiC layer on a 4 in. Si wafer at the low temperature of 1000°C without using a buffer layer. N-type epitaxial doping was performed and the I-V characteristic of the heterojunction diode n-SiC/p-Si was investigated.

Experimental

A cold-wall type reactor was used for growth. The schematic of the reactor is shown in Fig. 1. The substrates were 4 in. diam Si wafers with an orientation of 4°-off (111) toward $\langle 211 \rangle$ (hereafter noted as (111) 4° off). A substrate wafer was placed on a SiC-coated graphite susceptor, which was inductively heated at 8 kHz. This low frequency solves problems associated with plasma generation which occurs at low pressures.

Trichlorosilane (SiHCl_3) and propane (C_3H_8) were used as source gases for Si and C, respectively. H_2 was used as a carrier gas, and PH_3 was used as an n-type doping gas when necessary. Their flow rates were regulated by mass flow controllers. Since SiHCl_3 is a liquid, it was bubbled with H_2 using a Tylan Source V bubbler. A portion of the bubbled mixture was introduced into the reactor through a mass flow controller to get good controllability of the actual flow rate. We calculated the actual amount of SiHCl_3 introduced in the gas phase from the $\text{SiHCl}_3/\text{H}_2$ mole ratio measured by the Source V and the flow rate which was known from the substantial increase in pressure upon introduction. To exhaust the system, we used a series combination of a rotary and a mechanical booster pump which produced a pumping speed of 8×10^3 l/min. Nitrogen ballasting controlled the actual pumping speed to produce a

growth pressure of 200 Pa. The temperature was measured by a pyrometer through a quartz reactor tube and controlled at 1000°C except for experiments on temperature dependence. The temperature program is shown in Fig. 2. A prebake time of 10 min was adequate to obtain a clean substrate surface. Table I summarizes the conditions that we used in this experiment to grow single crystalline SiC layers.

We evaluated various properties of the grown films. We optically determined the thickness of the SiC film from peak and valley wavelengths in a reflectivity spectrum, assuming the SiC refractive index of 2.6 at wavelengths below 1000 nm. This method was valid for determining a thickness of a few hundred nanometers. The surface mor-

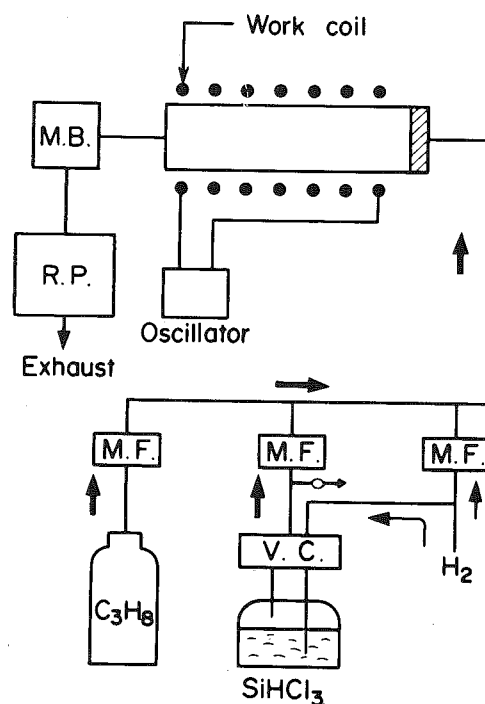


Fig. 1. Schematic of experimental setup. V.C., vaporizer controller; M.F., mass flow controller; M.B., mechanical booster pump; R.P., rotary pump.

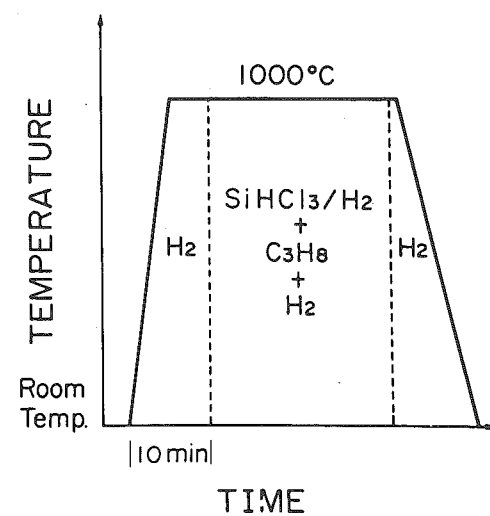


Fig. 2. Temperature program

phology was evaluated with a Nomarski differential microscope. For crystallographic evaluations, we used the x-ray diffraction and the reflection high energy electron diffraction (RHEED). In order to directly observe a lattice image of the β -SiC/Si interface, we took a cross-sectional transmission electron microscope (TEM) image.

We epitaxially doped the SiC films using PH_3 (phosphine). The sheet resistivity was measured for the doped n-type SiC layer grown on a p-type Si substrate with a 10 Ω -cm resistivity. The phosphorus concentration of the grown SiC layer was measured by the secondary ion mass spectroscopy (SIMS). In order to investigate the current-voltage characteristics of a single-crystal n-SiC/p-Si heterojunction, we fabricated a diode as shown in Fig. 3. We prepared a p-type (5 Ω -cm) substrate wafer which was implanted with boron ions at a dose of $1 \times 10^{15} \text{ cm}^{-2}$ at 100 keV through 200 nm thick Si_3N_4 and 20 nm thick SiO_2 and annealed at 900°C for 30 min. We used the Si_3N_4 layer to form a smooth surface which could not be obtained with a SiO_2 layer alone. The PH_3 flow rate was 2 cm^3/min to grow the n-SiC layer. NF_3 plasma successfully etched the SiC layers with a selectivity above 50 with aluminum electrodes as masks.

Results

Figure 4 is a photograph of β -SiC grown on a 4 in. (111) 4°-off Si substrate wafer. The thickness uniformity was $\pm 5\%$ excluding an area 10 mm from the wafer edge. As-grown surface morphology was mirror-like and unchanged after being dipped into molten KOH for a few minutes. No particular morphologies showing antiphase boundaries were observed. Figure 5 plots the growth rate vs. the C_3H_8 flow rate. The growth rate saturated at high C_3H_8 flow rates above 50 cm^3/min . The point of saturated growth rate increased almost linearly as the amount of SiHCl_3 was increased.

Figure 6 shows an x-ray diffraction pattern for a SiC layer on a Si (111) 4°-off substrate, together with that for a (100) substrate for comparison. There is a marked difference between results for the two orientations. The curve for the (111) 4°-off substrate shows only (111) and (222) β -SiC peaks with a very weak (111) Si substrate peak, while the curve for the (100) substrate shows an extra (111) peak with regular (200) and (400) β -SiC peaks. These results indicate that a single crystalline β -SiC layer grows on off-axial (111) substrates but not on (100) substrates. In addition, we

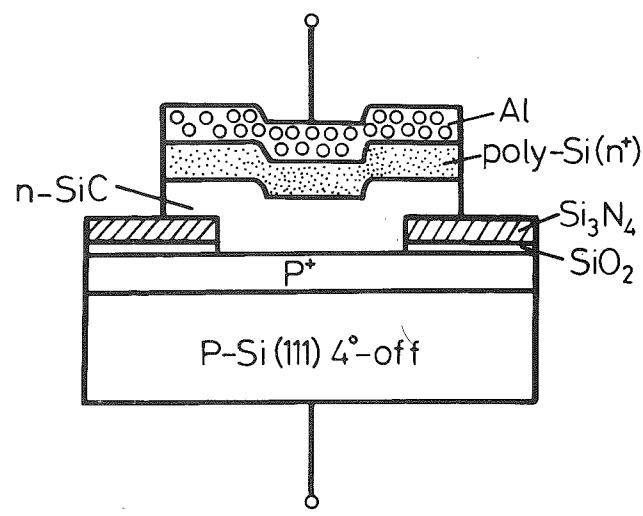
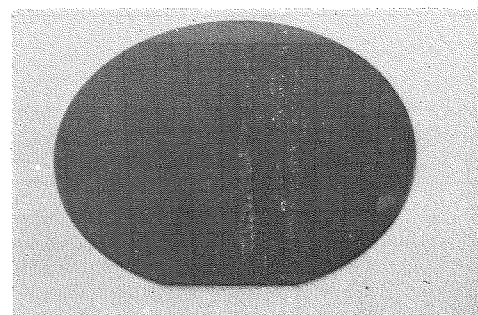
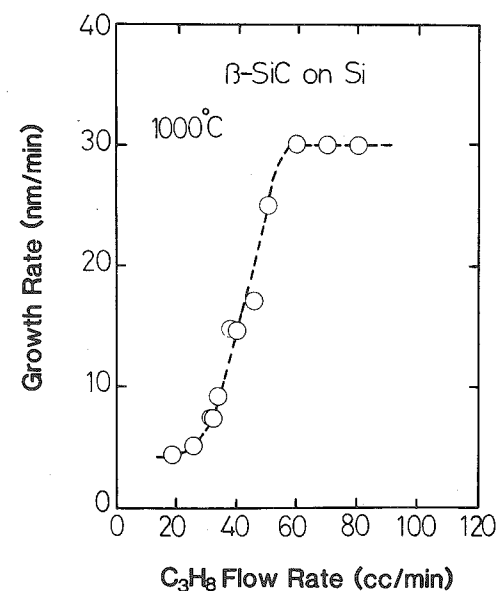


Fig. 3. SiC/Si heterojunction diode structure

Fig. 4. A photograph of β -SiC growth on a 4 in. off-axial (111) Si substrate.

found that the crystallinity depended on the flow rate of the source gases. X-ray analysis revealed that single crystalline β -SiC did not grow even on an off-axial (111) substrate if the flow rates of the source gases were too low. In fact, one third of the standard flow rates listed in the Table I did not yield a single crystalline layer.

Figure 7 shows a RHEED pattern for a β -SiC layer which was grown on a Si (111) 4°-off substrate. We can see streaky spots which indicate that the obtained SiC layer is a single crystalline layer with a smooth surface. Since the x-ray and RHEED evaluations proved that the obtained SiC was a single crystal, the next evaluation was to examine the lattice image around the SiC/Si interface.

Fig. 5. Growth rate as a function of C_3H_8 flow rateTable I. Standard conditions for β -SiC growth

Gas flow rates (l/min)	
H_2	7.0
SiHCl_3	0.70
C_3H_8	0.040
Temperature (°C)	1000
Pressure (Pa)	200

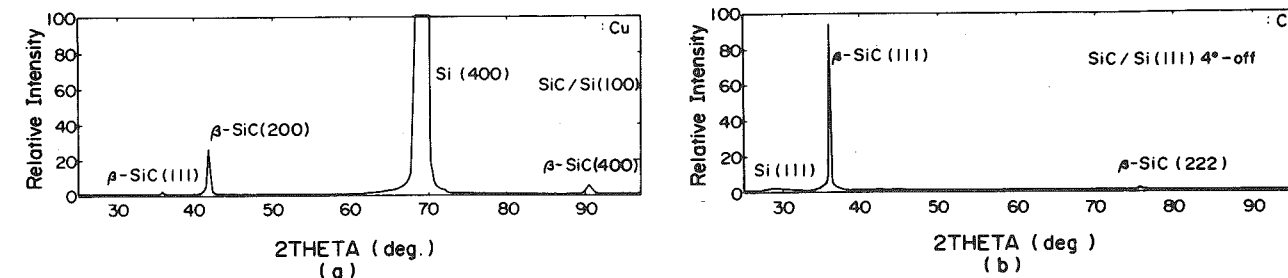


Fig. 6. X-ray diffraction patterns

Figure 8 shows a cross-sectional TEM image of the β -SiC/Si interface. We can directly observe the lattice image of the β -SiC (111) planes which are stacked a quite orderly way on the Si (111) 4°-off substrate. However, we often found disordered parts in the lattice image. We also found dark parts which pass the SiC layer.

Figure 9 shows the sheet resistivity and phosphorus concentration as a function of PH_3 flow rate for a 400 nm thick β -SiC layer. The sheet resistivity decreased and, correspondingly, the phosphorus concentration increased as the PH_3 flow rate exceeded about 1 cm^3/min , the sheet resistivity and the phosphorus concentration were saturated. In order to investigate phosphorus diffusion into the substrate during growth, we measured the phosphorus concentration profile across the interface. The result is shown in Fig. 10. The phosphorus impurities distributed uniformly in the SiC layer and did not diffuse into the Si substrate within the SIMS resolution of about 10 nm. This result confirms that the simple product of film thickness and sheet resistivity will give the specific resistivity of the film. Then, we get a saturated specific resistivity of $3 \times 10^{-2} \Omega\text{-cm}$ from the result in Fig. 9. The saturated phosphorus concentration in the SiC layer was $2 \times 10^{20}/\text{cm}^3$ which was measured by the SIMS with calibration using p^+ implanted SiC references. The SiC/Si sharp junction tells us that β -SiC grown by this technique can be used as a wide gap material in Si heterojunction devices. From this view point, we investigated the current-voltage characteristics of a diode between an epitaxial n-SiC and p-Si substrate. The results are shown in Fig. 11. The forward current is generally modeled by $\exp(-qV/nkT)$, where n is the diode ideality factor related to the conduction mechanism. We derived a value of 1.05 ± 0.05 for n from the results in Fig. 11, indicating that the dominant current component is a diffusion current. The leakage current was about 10^{-11} A at a reverse bias of 0.6V.

Discussion

This paper has described the growth of a single crystalline β -SiC layer on a Si substrate at 1000°C without using a buffer layer. The growth at the temperature of 1000°C is progress in the SiC-on-Si heteroepitaxy technology because the low temperature growth is slip line free even on a 4 in. wafer and without contamination from the growth circumstances. We also found that the direct SiC/Si junc-

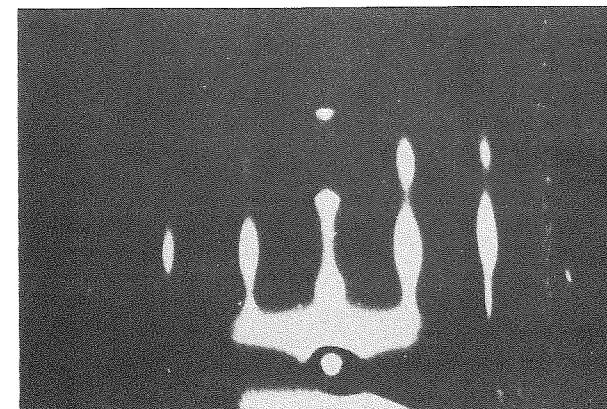
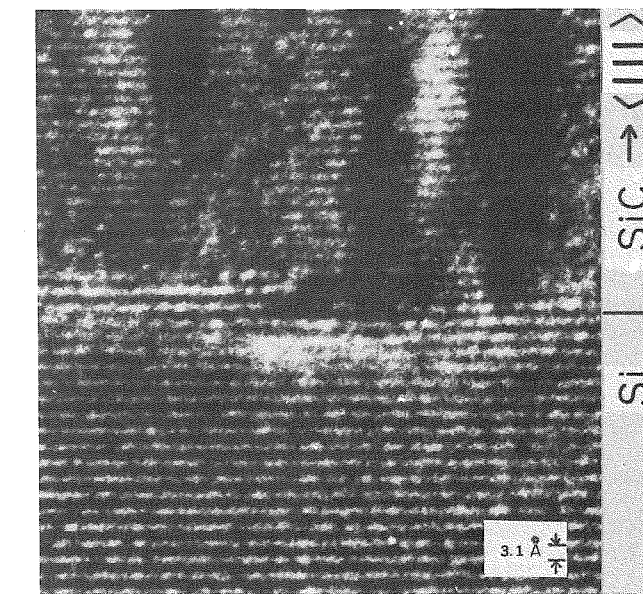
Fig. 7. RHEED pattern for a grown β -SiC layer

Fig. 8. Cross-sectional TEM lattice image

tion without a buffer layer produced a diode factor of 1.05 whereas the crystal SiC/Si system has a lattice mismatch of 20%. These results encourage us to look for unconventional applications for the SiC/Si heterojunction devices which have new capabilities. Before we develop those devices, we should know the mechanism that describes its growth. We have some phenomena that distinguish this heteroepitaxy from the other types of SiC/Si growth reported previously. Therefore, we would like to discuss these phenomena and their relationship to the growth mechanism.

This heteroepitaxy uses some specific conditions. They include a pressure of 200 Pa and a temperature of 1000°C. The low pressure eventually produces a high linear velocity which achieves a thinner stagnant layer than that in atmospheric-pressure growth. A stagnant layer formed just above a substrate is effectively heated by heat conduction from the susceptor, and the zone outside the stagnant layer is not heated very effectively. Therefore, the low pressure limits the heated zone to the stagnant layer which is very close to the substrate surface. The source gas in the heated zone generates reactive species. It is well known that the $\text{SiHCl}_3\text{-H}_2$ system heated at high temperatures generates very reactive species of SiCl_2 which strongly enhances Si nucleation or growth on the substrate (5, 6). However, its equilibrium partial pressure at 1000°C is so low compared with the other species of SiH_2Cl_2 , SiHCl_3 , and HCl (7) that the SiCl_2 associated nucleation may be rare under these conditions. We believe that the species which contribute most to Si nucleation is the undissociated SiHCl_3 which has a much higher partial pressure than the other species under this high linear velocity (400 cm/s). A similar thing can be said for carbon nucleation from a $\text{C}_3\text{H}_8\text{-H}_2$ system. The species produced by thermal cracking will include C_2H_2 and C_2H_4 . But, under this high linear velocity, the dominant species in nucleation will still be the undissociated C_3H_8 . We propose here that species involved in this heteroepitaxy are undissociated SiHCl_3 and C_3H_8 which

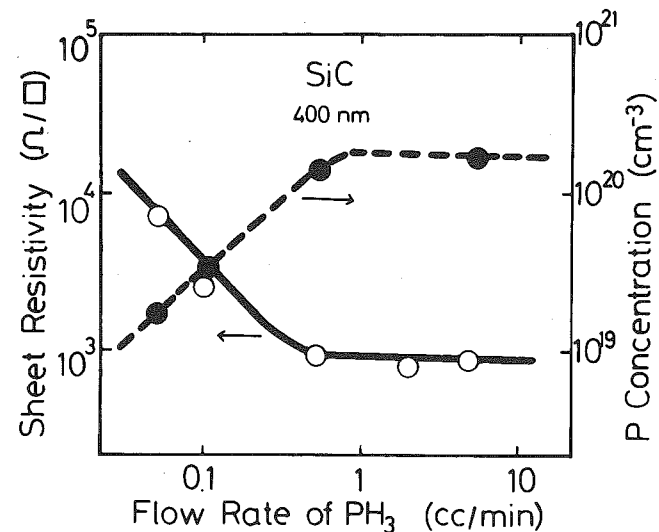


Fig. 9. Sheet resistivity and phosphorus concentration as a function of PH_3 flow rate.

will be relatively inert compared with the dissociated radicals. When inert species are mainly involved in the growth, nucleation properties are very much affected by the substrate surface. In other words, nucleation is influenced or determined by surface elements. Thus we will first discuss the nucleation of Si and C.

It is obvious that Si nucleation takes place easily on a Si substrate from a $\text{SiHCl}_3\text{-H}_2$ system because Si homoepitaxy took place in our experiment. We also found that Si nucleation did not take place in the same system on special areas of the substrate which were intentionally contaminated with carbon. We call these areas epitaxial defects or dimples. These defects are a result of Si surface changes which the carbon contamination or carbonization caused. The result indicates that Si nucleation occurred easily on a Si surface while not on a carbon-contaminated surface. The next question is whether carbon will nucleate on Si substrates. We examined the carbon nucleation by subjecting a Si substrate to a $\text{C}_3\text{H}_8\text{-H}_2$ system at 1000°C . The results are shown in Fig. 12. After 2 min, the surface became rough due to local carbonization, accompanying hillocks. But, after 10 min, the surface became smooth again because of the complete carbonization. However, carbon growth did not occur even for further subsection. We verified the surface carbonization for the 10 min sub-

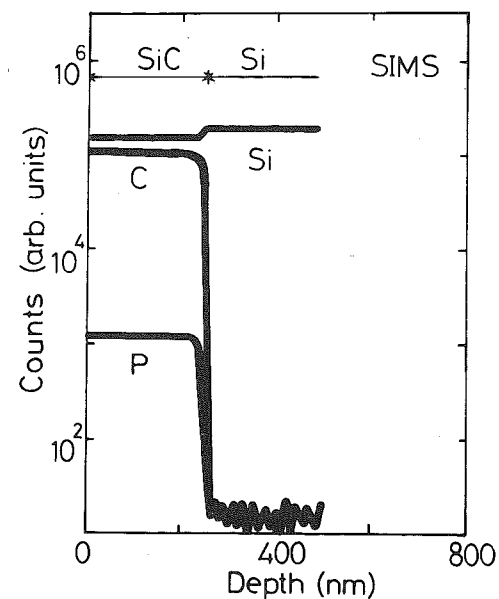


Fig. 10. Concentration profiles for depth of Si, C, and P

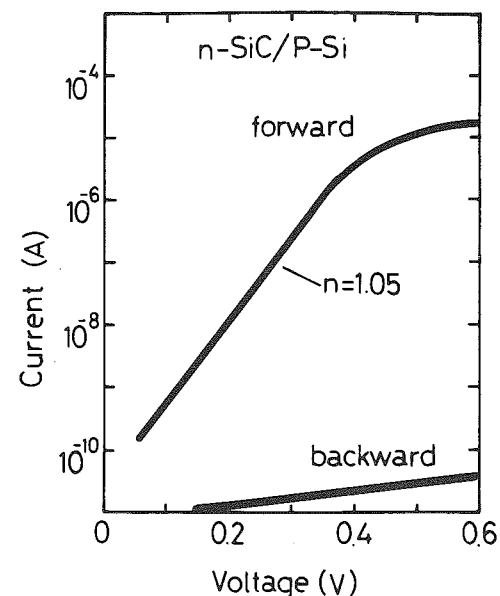


Fig. 11. Current-voltage characteristics for an n-SiC/p-Si heterojunction diode. The n-SiC layer was 60 nm thick and had a resistivity of $3 \times 10^{-2} \Omega\text{-cm}$. The p-Si layer was formed by 10^{15}cm^{-2} dose B^+ implantation to a 5 $\Omega\text{-cm}$ Si substrate and a subsequent 900°C annealing.

jection with energy loss spectroscopy (ELS) and x-ray photoelectron spectroscopy (XPS). The ELS observed the plasmon loss peak at an energy loss of about 20 eV which stands for the SiC crystal (Fig. 13). The XPS spectrum showed C_{1s} peak at about 283 eV with a chemical shift of Si-C bond, accompanying a subsidiary peak of free C which disappeared after surface sputtering with Ar ions (Fig. 14). These results show that the carbonization takes place at the Si surface. The same examinations were performed for Si and C nucleation on SiC layers which were grown with conditions listed in Table I. The Si nucleations took place at a density of $10^4\text{-}10^5/\text{cm}^2$ with many large areas left un-nucleated. The nuclei grew with time finally to cover the wafer surface. The carbon nucleation test did not cause any changes in the SiC surface appearance. We conclude from these nucleation examinations at 1000°C that Si does not nucleate properly against a carbonized Si surface or a SiC surface from a $\text{SiHCl}_3\text{-H}_2$ system and carbonization does take place on Si substrate surfaces which are subjected to a $\text{C}_3\text{H}_8\text{-H}_2$ system.

Since we have investigated the nucleation of Si and C separately, we will now discuss the growth mechanism of this heteroepitaxy using the actual $\text{SiHCl}_3\text{-C}_3\text{H}_8\text{-H}_2$ gas system. Nucleation of Si and C must continuously and simultaneously take place in the actual system for SiC growth along the $\langle 111 \rangle$ direction. The first step in the growth process will be the carbonization of a Si substrate surface. The next step must be the Si nucleation for the SiC growth. However, this rarely takes place as discussed previously. In order to answer this question, we propose that the Si atoms or undissociated SiHCl_3 molecules migrating on the carbonized surface are promptly carbonized again and SiC monolayers are easily formed. Given this assumption, the top surface of the grown SiC is always terminated by the

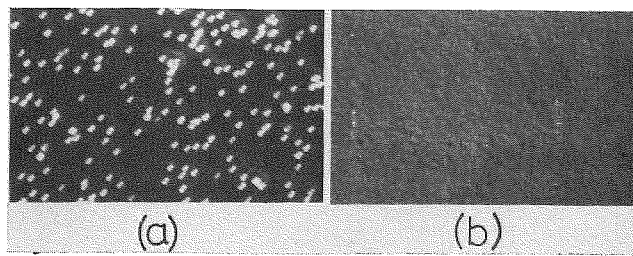


Fig. 12. Microscope photographs for Si substrate surfaces which were carbonized for (a) 2 min and (b) 10 min with $\text{C}_3\text{H}_8\text{-H}_2$ at 1000°C .

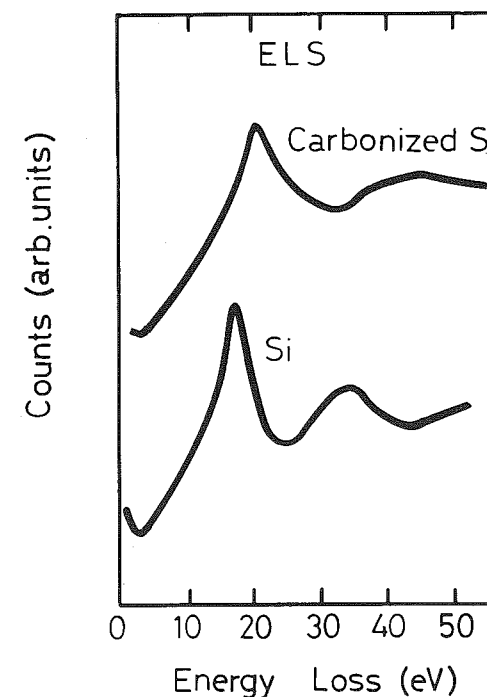


Fig. 13. ELS spectra for Si wafer surface with and without carbonization which was performed at 1000°C for 10 min with a $\text{C}_3\text{H}_8\text{-H}_2$ gas. E_p was 2000 eV.

carbon atoms. This coincides fairly well with the experimental finding that Si hardly grows on SiC surfaces on which the Si layer should grow if the SiC surface is otherwise terminated.

While we understand the process of continuous SiC growth taking into account prompt carbonization of the Si atoms or Si carrying species which are on the carbonized Si substrate, there is a possibility that Si-Si bonds may form stacking faults and cause deviation from the stoichiometric composition which were not observed. A mechanism to crack these bonds must be considered to explain the single crystalline growth. The results in Fig. 12, 13, and 14 indicate that the carbonization is very reactive and can reach into the growing SiC layer, suggesting that surface Si atoms might be easily replaced by penetrating carbon atoms. This very strong carbonization successfully explains the complete Si-C bond formation, excluding the Si-Si bond formation. This implies that the stoichiometry is automatically satisfied as long as the carbonization is sufficiently strong. This provides an operating margin for the gas flow control which will be very helpful for practical fabrication.

Having discussed nucleation, next we discuss the crystal defects. The misfit dislocation density is expected to be very high because the lattice mismatch is 20% between SiC and Si. However, the as-grown surface had mirror morphology although we have observed dark parts in the TEM image which will be related to dislocations or strained field that the lattice mismatch induced in the SiC layer. The molten KOH dip did not cause any particular etch pits. If the dislocations are produced at the calculated density, etch pits will be observed correspondingly. Moreover, the misfit energy at the interface between the two crystals will be very large and inhibit a stable heteroepitaxy. It is a reasonable understanding that a single crystalline SiC cannot grow on a Si substrate with an extremely high dislocation density and without a relaxing mechanism. We found that the SiC layer peeled off the Si substrate when it was grown at more than 1100°C . This indicates that SiC directly grown on Si can be unstable, depending on the growth conditions. However, we have grown single crystalline $\beta\text{-SiC}$ on Si without peeling at 1000°C . We need a model to explain this successfully. But, we have now no specific model. We think that a kind of the intermediate layer or buffer layer may exist probably due to oxygen impurities or residual

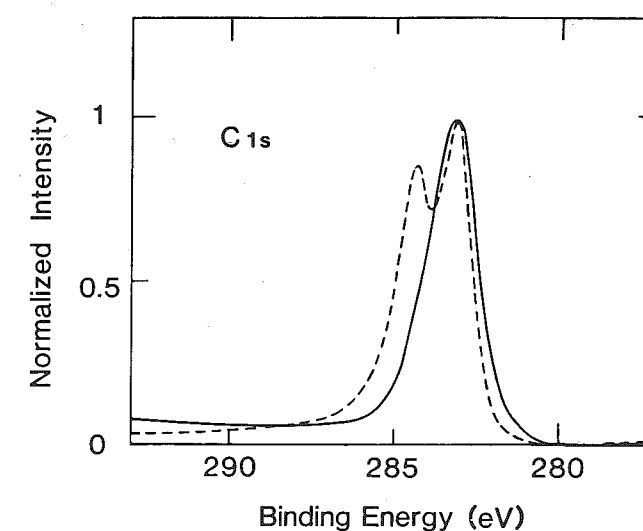


Fig. 14. XPS spectra for carbonized Si wafer surfaces with (solid curve) and without (dashed curve) Ar-sputtering. The subsidiary peak for free carbon disappeared after the sputtering.

silicon oxide, which SIMS measured. Such a buffer layer will relax the interface misfit energy and prevent the peeling. Further experiments are necessary to interpret the lattice structure at the interface including the electrical characteristics.

This heteroepitaxy has another particular characteristic which is the off-axial wafer substrate. This factor was decisive in obtaining a single crystalline $\beta\text{-SiC}$ layer (see Fig. 6). It is already known that substrate orientation influences the crystallinity in heteroepitaxial growth (8-10). Generally speaking, steps of an atomic order are formed at the surface when a Si substrate is heated. Off-axial (111) substrates have the merit that steps with a height of a two-atomic layer tend to form with a density corresponding to the off-angle. This is because Si (111) planes are separated with two different distances, and make plane pairs. These (111) pairs are stable at high temperatures and they will form surface steps on off-axial (111) substrate wafers. These are called biatomic steps. If the biatomic steps cover the substrate surface, a favorable mechanism will dominate SiC growth as in GaAs-on-Si heteroepitaxy. In other words, antiphase generation can be avoided since the stacking order of Si and C (111) planes are not disturbed by the step-height difference.

Our next concern is the off-angle. We consider the off-angle to have a strong influence on surface morphology. When the surface diffusion length is long compared with step-to-step distances, lateral growth will dominate, leading to a very smooth surface morphology. When the diffusion length is shorter than the step-to-step distances, nucleations may occur at many locations on the terrace, often leading to a coarse morphology. Therefore, the step-to-step distance should be short to achieve a smooth morphology for a given diffusion length. Roughly speaking, the 4° off-angle gives a step-to-step distance of about 5 nm on a Si (111) surface. Since we obtained a smooth morphology, the diffusion lengths of the species involved are longer than 5 nm. Although the off-angle of 4° in this experiment is twice as large as 2° which Liaw and Davis obtained with a two-step growth procedure (11), we think that the proper off-angle may depend upon the specific growth mechanism.

Figure 10 shows that the phosphorus does not diffuse into the substrate during growth within the limits of the SIMS resolution, resulting in an abrupt n-SiC/p-Si heterojunction. This implies that the SiC layer blocks phosphorus diffusion into the substrate from the vapor phase. The blocking ability increases as the thickness of the SiC layer increases. This property may be a great advantage in making devices which require an abrupt junction.

Next we discuss the electrical properties. The phosphorus-doped SiC showed a saturation characteristic in the sheet resistivity and the phosphorus concentration for

high flow rates of PH_3 (see Fig. 9). This saturation probably comes from a thermodynamical property or solubility limit of the phosphorus at a given temperature. The saturated phosphorus concentration is $2 \times 10^{20}/\text{cm}^3$ which is much larger than $1 \times 10^{19}/\text{cm}^3$ reported by Davis *et al.* (12). The difference will be related to the growth condition difference between the two. The ratio of carrier concentration to total phosphorus concentration was a few percent. This is low compared with 0.1% reported by Davis *et al.* (12). Since the impurity ionization depends on all the properties the crystal has, the detailed discussion requires further study on SiC crystal. An n-SiC/p-Si heterojunction diode yielded a diode factor of 1.05 which was much better than we had expected with the large lattice mismatch of 20% between SiC and Si. Generally speaking, the recombination center density increases with increase in the dislocation density induced by lattice mismatch. If dislocations are introduced at a density corresponding to the mismatch, the diode factor which we obtained is too good. In addition to the dislocation density, we must take into account the autodoping of the boron impurity from the p-Si substrate in order to correctly evaluate the heterojunctions. Solving these problems will require more detailed research on the crystallography of the SiC/Si system.

Conclusion

We grew single crystalline β -SiC layers directly on Si substrates with an off-axial (111) orientation. This heteroepitaxy was performed at 1000°C, 200 Pa, and with SiHCl_3 - C_3H_8 - H_2 system which provided favorable conditions for obtaining stoichiometry in the SiC layer. A heterojunction

diode was fabricated by growing a phosphorus doped n-SiC layer on a p-Si substrate. This diode showed an ideality factor of 1.05.

Acknowledgment

We thank T. Sugii and T. Ito of Fujitsu Laboratories Limited for their fruitful discussions, and process development director K. Yanagida for his encouragement.

REFERENCES

1. D. F. Ferry, *Phys. Rev. B*, **12**, 2361 (1975).
2. H. Matsunami, S. Nishino, and T. Tanaka, *IEEE Trans. Electron Devices*, **ED-28**, 1235 (1981).
3. S. Nishino, H. Suhara, and H. Matsunami, in *Extended Abstracts of 15th Conference on Solid State Devices and Materials*, Tokyo, p. 317 (1983).
4. K. Sasaki, E. Sakuma, S. Misawa, S. Yoshida, and S. Gonda, *Appl. Phys. Lett.*, **45**, 72 (1984).
5. W. A. P. Claassen and J. Bloem, *This Journal*, **127**, 1836 (1980).
6. J. Nishizawa and H. Nihira, *J. Cryst. Growth*, **45**, 82 (1978).
7. L. P. Hunt and E. Sirtl, *This Journal*, **119**, 1741 (1972).
8. K. Shibahara, S. Nishino, and H. Matsunami, *J. Cryst. Growth*, **78**, 538 (1986).
9. R. Fisher, H. Morkoc, D. A. Neumann, H. Zabel, C. Choi, N. Otska, M. Longerbone, and L. P. Erickson, *J. Appl. Phys.*, **60**, 1640 (1986).
10. H. Kroemer, *Proc. MRS*, **67**, 3 (1986).
11. P. Liaw and R. F. Davis, *This Journal*, **132**, 642 (1985).
12. R. F. Davis, H. Kong, J. A. Edmond, and J. T. Glass, in *Abstracts of MRS Spring Meeting*, p. 273 (1987).